SSCL-Preprint-192

SSCL-Preprint-192
February 1993
Distribution Category: 400

M. Diwan

Design of a Compact Beam Dump for the BNL-AGS Neutral Beam

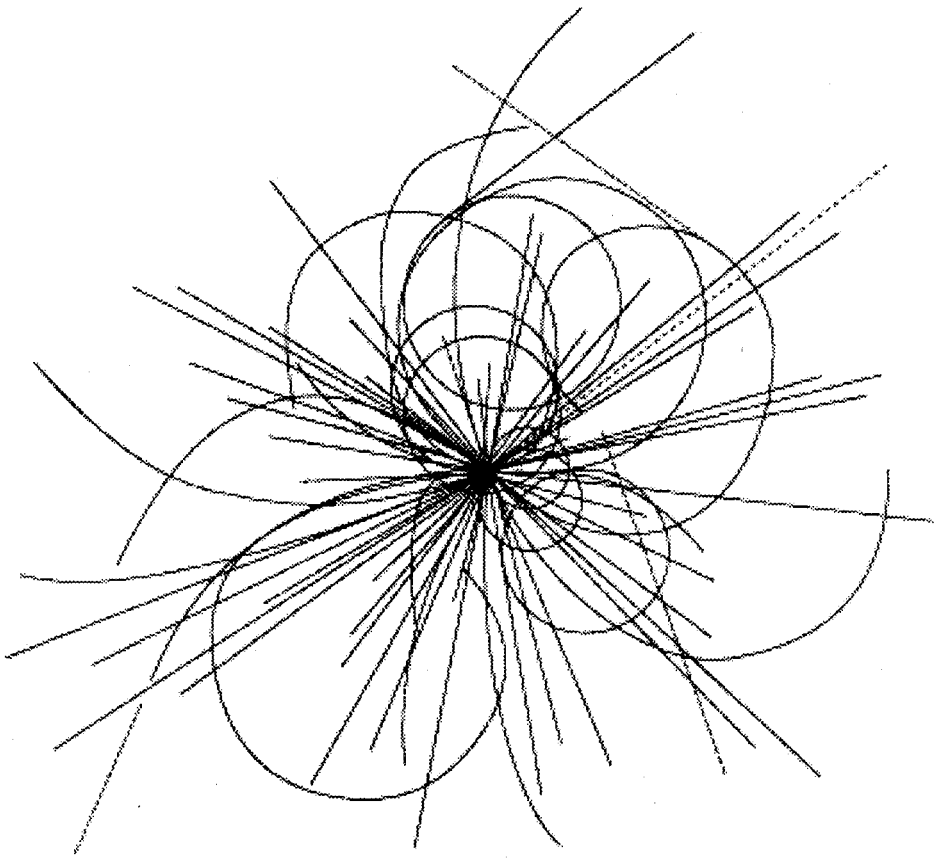

Superconducting Super Collider Laboratory

SSCL-Preprint-192

Design of a Compact Beam Dump for the BNL-AGS Neutral Beam*

M. Diwan

Superconducting Super Collider Laboratory†
2550 Beckleymeade Ave.
Dallas, TX 75237

February 1993

*Presented at the Simulating Accelerator Radiation Environments Workshop held at Los Alamos National Laboratory, January 11–15, 1993.

†Operated by the Universities Research Association, Inc., for the U.S. Department of Energy under Contract No. DE–AC35–89ER40486.

DESIGN OF A COMPACT BEAM DUMP FOR THE BNL-AGS NEUTRAL BEAM.

Milind Vaman Diwan
Stanford University, Department of Physics, Stanford, CA. 94309
and
Physics Department, Superconducting Super Collider Laboratory, Dallas, Texas 75237-3946

INTRODUCTION

BNL-E871 is a two arm rare kaon decay spectrometer at the BNL-AGS [1]. The experiment uses a neutral kaon beam to search for the forbidden decay $K_L^0 \rightarrow \mu e$. The previous experiment (E791 [2]) in the same beam line allowed the neutral beam to pass through a gap in the spectrometer. For E871 it seems more advantageous to dispose of the beam in a compact beam dump located in the middle of the spectrometer. The elimination of the beam allows increase in acceptance by eliminating the gap in the downstream spectrometer, reduces accidentals in the trigger, and in the downstream particle identification detectors. Fig. 1 is a schematic of the E871 detector.

GENERAL CONSIDERATIONS

The neutral beam for E871 is produced by 24 GeV/c primary protons incident on a copper target. Secondary particles produced at 48 mrad in a 65 μsr solid angle are collimated into the kaon detector. Charged particles and photons are eliminated using lead foils and sweeping magnets to produce a neutral beam composed of neutrons and neutral kaons. The neutron to kaon (n/k) ratio is estimated to be between 12-24 [3]. It has been estimated that there are about 3.5×10^8 neutrons in the beam for every 10^{12} (TP) protons on the primary target. The neutron spectrum is broad with a mean energy of 10 GeV and a maximum of 20 GeV [4]. The compact beam dump then must absorb the neutral beam without producing secondary radiations that produce hits in the surrounding detectors.

The space available for the beam plug (0.4 m in the magnet bend view and 2.5 m along the beam. See Fig. 1) is limited by acceptance considerations for $K_L^0 \rightarrow \mu e$. The following general considerations about the processes generating radiations out of the plug along with much experimentation led us to the plug design shown in Fig. 2. After the primary high energy cascade in dense matter photons, charged particles, and neutrons from nuclear boil off are left over. With sufficient density and thickness of material the charged particles and photons should get absorbed within the plug. The neutrons from nuclear boil off tend to be in the 1-20 MeV range.

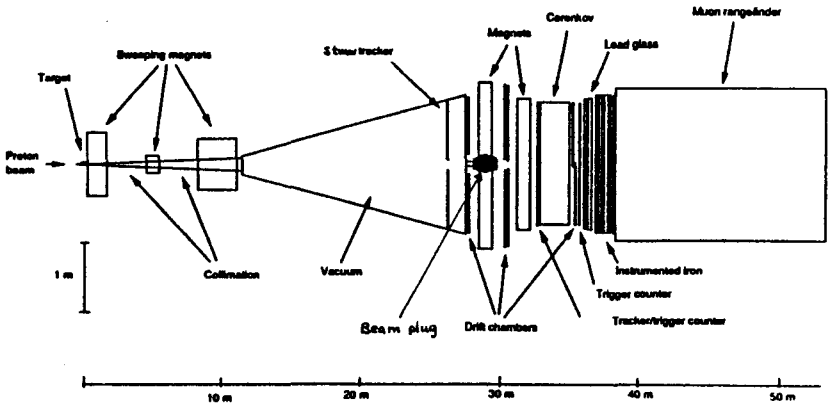

Fig. 1. Plan view of the E871 apparatus

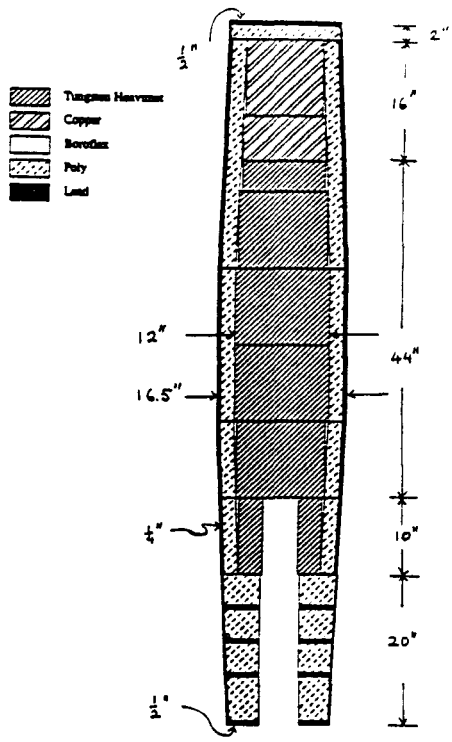

Fig. 2. Plan view of the fully shielded beam plug. The central section of tungsten was 28" high with 3" copper and 5" polyethylene above and below the tungsten. This height completely filled the vertical gap of the magnet. Boroflex has 30% boron content. The other polyethylene had 0.5% boron content.

Multiple neutron production (and fission in the case of uranium) and inelastic (n,n′) cross sections are important in this region. Though these processes generate extra neutrons they are effective in degrading neutron energies. As the neutron is degraded below 100 KeV the most effective neutron removal process is (n,γ) reaction. Unfortunately (n,γ) cross sections are not high enough to rapidly remove neutrons in the 100 KeV range in practical high density materials. Some low Z materials have appreciable (n,p) or (n,α) cross sections, but do not have the density required for short mean free paths. Thus we are forced to rapidly thermalize these neutrons and absorb them on nuclei with very high absorption cross sections at thermal energies. This naturally leads us to use materials with the highest possible hydrogen density.

These consideration led us to use tungsten as the core of the beam plug and borated polyethylene as the neutron absorber. Tungsten has higher cross section for the inelastic processes than lead or uranium [5]. It is also very dense (we used an alloy of tungsten, heavimet, with density of 18.5 gm/cc, but pure tungsten has density of 19.3 gm/cc) and user friendly. Borated polyethylene (CH_2) was the material of choice surrounding the plug for thermalization and capture of escaping neutrons. The density of downstream material was not considered critical because the main hadronic cascade should end in the tungsten core which is about 10 interaction lengths long. Thus the purpose of the downstream material (copper) was to absorb charged tracks escaping the front of the plug.

EXPERIMENT

The beam plug described in the previous section was tested in the 1990 run at the AGS. The test setup is shown in Fig. 3. The test was performed using the previous experimental setup, E791. The plug was located in the second magnet (96D40). Configuration of the plug, the surrounding material, and the magnetic field were changed from run to run to get a detailed understanding of the counting rates in the detectors. 88 different configurations were tested before arriving at the final configuration. These data are tabulated in internal collaboration notes and will be published [6], but here we will only describe a selected set of measurements.

There were two different sets of detectors used for the measurements. The E791 drift chambers, scintillation counters, and particle identification detectors were used to determine the counting rates expected in similar detectors that will be used in E871. Specialized detectors such as

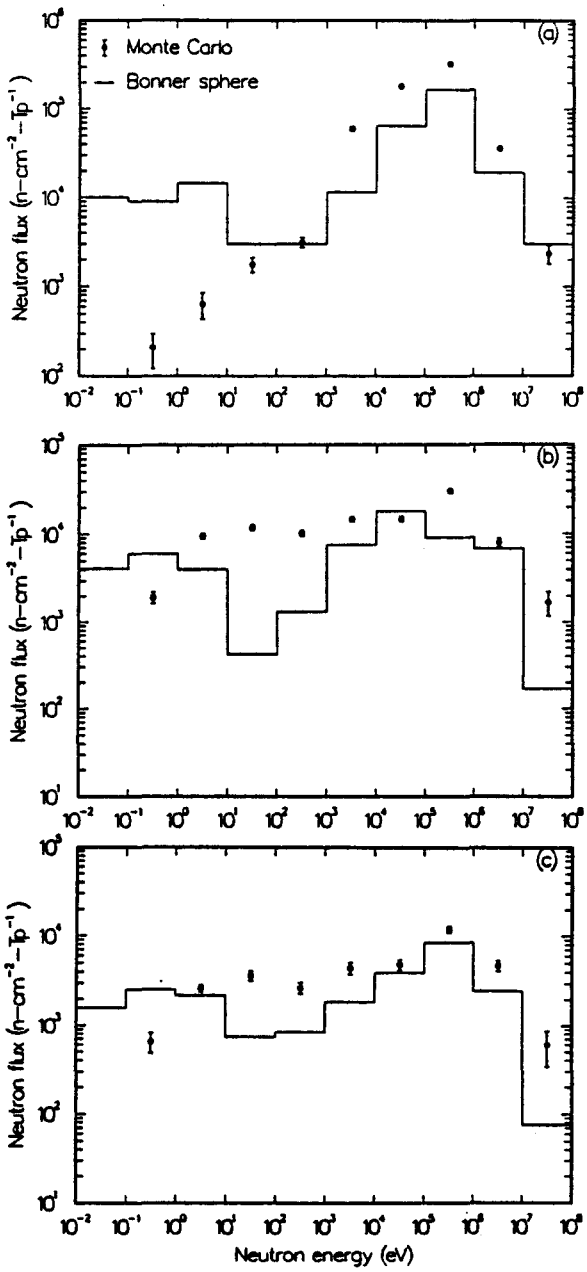

Fig. 4. Comparison of Monte Carlo predicted neutron spectrum and measurements using Bonner spheres at the position of the upstream drift chamber for (a) metal only plug, (b) shielded plug, and (c) plug with an extra inch of tungsten and polyethylene.

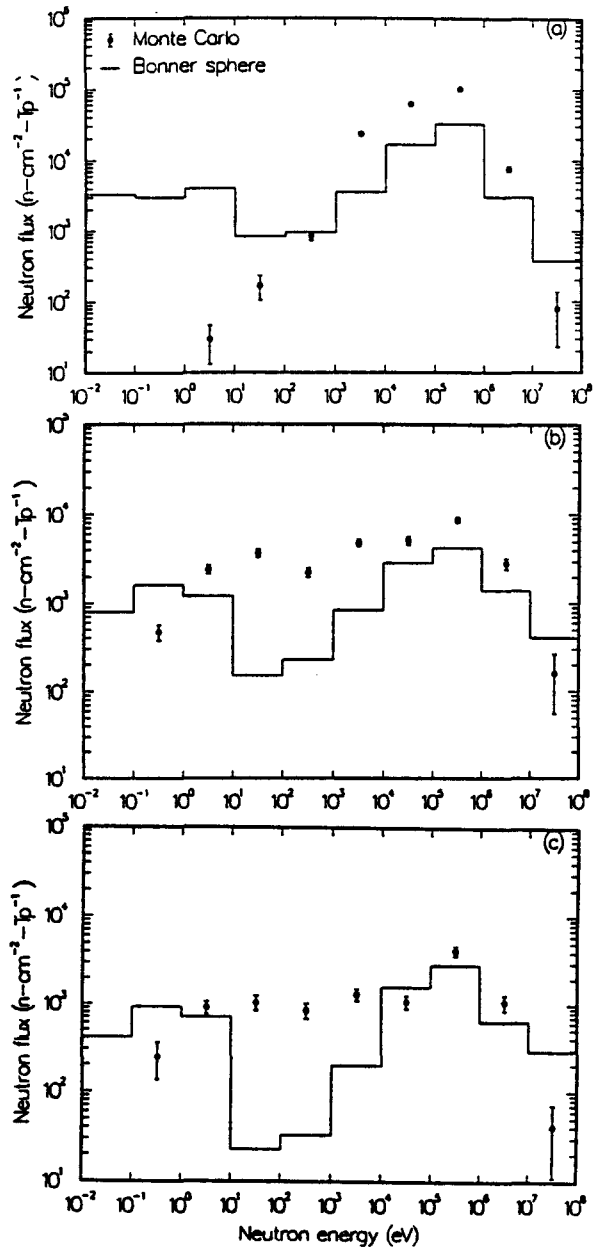

Fig. 5. Comparison of Monte Carlo predicted neutron spectrum and measurements using Bonner spheres at the position of the downstream drift chamber for (a) metal only plug, (b) shielded plug, and (c) plug with an extra inch of tungsten and polyethylene.

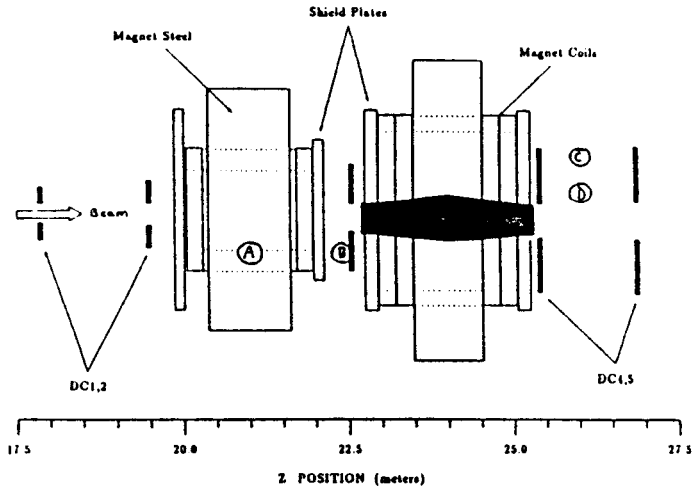

Fig. 3. Schematic of the test setup. A, B, C, D are the positions of the special detectors that were used to find neutron, photon, and charged particle fluxes. Positions B and D were used for the Bonner sphere measurement. All four positions were used for the liquid scintillator measurements. The E791 scintillator hodoscope and particle identification counters (Cerenkov, lead glass, muon range finder) were located downstream of DC5.

Bonner spheres, a small cell of liquid scintillator surrounded by plastic scintillator paddles, ^{3}He counters, as well as a germanium detector were used to get a more fundamental understanding of the neutron, photon, and charged particle fluxes coming out of the plug. In the following paragraphs we briefly describe some of the measurements.

Bonner Spheres

The Bonner sphere [7] is a moderated neutron detector. The detector is a 4 mm × 4 mm cylindrical LiI(Eu) scintillating crystal located at the center of a polyethylene ball. The polyethylene ball degrades the neutrons which are detected by the reaction ^{6}Li(n,α)^{3}H. The signal is read out by a PMT attached through a light pipe and digitized by an ADC. The ADC distribution is fitted to subtract background from charged particles passing through the scintillator. We had polyethylene moderators of six different diameters, 2", 4", 5", 8", 10", and 12". These six, the bare detector, the detector wrapped in cadmium, and the 2" ball wrapped in cadmium make a total of 9 configurations. Each of these configurations had a different energy response. Normalized counting rate was measured for each configuration and then the energy spectrum was unfolded using the tabulated energy response and the computer program BUNKI [8]. The neutron spectrum was measured for selected plug configurations and it is displayed in figures 4 and 5. The ^{3}He counter measurements were made unreliable due to pile up and wall effects. However, they served as a check on the Bonner sphere measurements.

Liquid Scintillator measurements

A liquid scintillator cell surrounded by two flat plastic scintillators was used to measure the higher energy neutron spectrum. The setup was also useful for measurements of photons and charged particles. The liquid scintillator was Bicron BC-501A in a cylindrical glass cell measuring 5 cm × 5 cm. A 5" aluminum can was placed around the cell to make it light tight. The plastic scintillators were 4" × 4" × 1/8", mounted on either side of the liquid scintillator, about 4" from its center. Neutrons interact with protons in the liquid scintillator leaving heavily ionizing pulses with long tails. Photons and charged particles interact with electrons

leaving pulses with faster decay times. A digital technique of pulse shape discrimination (PSD) was used to separate neutrons from photons [9]. Two ADC's were used for PSD, one integrated the rising part of the pulse and the other integrated the tail. The ratio of the two ADC's allowed easy discrimination of neutrons and photons above 0.5 MeV. The full ADC spectrum for well identified neutrons was unfolded using the program FERD [10] to get a spectrum between 0.9 and 7.0 MeV. The integrated spectrum agreed with the Bonner sphere results within a factor of two. The runs were taken at different times and with changing beam conditions and therefore this level of agreement was considered reasonable.

Photons and charged particles were also identified with the liquid scintillator setup. Photon and neutron separation using PSD failed at energies below 200 KeV. Photons were defined to have PSD consistent with minimum ionizing particles and neither plastic scintillator firing its discriminator. The discriminator threshold on the liquid scintillator was set at 125 KeV and therefore some neutron contamination exists in the photon rate. Charged particles were identified by requiring coincidence between both plastic scintillators and the liquid scintillator or coincidence between one of the plastic scintillators and the liquid scintillator having ADC measurement consistent with a charged particle. Table 1 lists these rates for selected configurations of the plug and for selected positions from Fig. 3.

Drift Chambers

The E791 drift chambers used in the experiment were hexagonal celled with (x,x′) and (y,y′) staggered geometry. The pitch, the distance between x and x′ wires, was 0.5 cm. The chambers were operated with a mixture of 50% argon and 50% ethane. The chambers had aluminum coated mylar skins (9μ Al, 13μ Mylar) [2]. Rates of single wire hits were measured in these drift chambers for many configurations of the plug and the magnetic field. Effort was also made to analyze the patterns of hits to understand the origin of the extra rate from the plug. Adjacent single wire hits were grouped together to form clusters of hits. And the singles rate was divided into rate due to clusters of various sizes. (1, 2, 3, or more than 3 wires). Fig. 6 shows such a categorization for drift chambers 3 and 4, upstream and downstream of the plug, respectively.

Other Detectors

A Germanium detector was used to measure the spectrum of photons in the 0.1 to 10 MeV range. Proper normalization could not be obtained for this measurement. Though the spectrum showed several well identified lines (477 KeV from $^{10}B(n,\alpha)^{7}Li$ with consequent decay of the ^{7}Li excited state and 2.22 MeV from n capture on hydrogen) most of the counts came from a continuous distribution that was peaked in the low energy range less than 200 KeV and decreased rapidly at higher energies.

The Cerenkov detector PMT's (5" diameter RCA Quantacon) showed a surprising increase in the singles rates at thresholds below 1 photoelectron. Locally shielding the PMT's with borated polyethylene and lead decreased these rates leading to the conclusion that the increased rates were caused by interactions in the PMT.

	n	γ	c	Plug Configuration
Position A	13.6	37.7	2.4	Bare Metal
Upstream	2.5	12.2	1.9	Fully shielded
	2.2	8.0	1.1	Copper extension to tunnel
Position D	2.3	13.0	1.0	Bare Metal
downstream	1.2	5.9	0.8	Fully shielded
nearer	2.2	3.6	1.1	Additional 1" W and 1" poly
Position C	3.6	13.4	0.8	Bare Metal
downstream	1.4	5.6	0.7	Fully shielded
farther	0.9	3.5	0.5	Additional 1" W and 1" poly

Table 1. Neutron, photon, and charged rates in the liquid scintillator setup for selected positions (Fig. 3) and plug configurations. The magnetic field was off for these measurements. The numbers are normalized to the beam telescope. The relative normalization is good to about 10%. Data was taken for many more intermediate configurations and with magnetic field on. The table illustrates the process by which we optimized the design of the plug.

ANALYSIS

The difficult part of the experiment was normalization. The absolute normalization (rate per beam neutron) was uncertain by 30% because of the uncertainty in the n/k ratio [3].

The relative normalization between runs was performed in two ways: The counts in a beam telescope (a scintillator counter located at 90° near the main copper target) were used to normalize the detector rates shown in this paper. The number of reconstructed Vee's using the front part of the spectrometer (DC1-DC2 Fig. 3) were also used for normalization of hit rates since they are proportional to the number of kaons in the neutral beam. These two methods of normalization agreed with each other within 20%, but the Vee's normalization suffered from lack of statistics. The relative normalization using the beam telescope is considered good to about 10%.

Understanding drift chamber rates was of prime importance since similar detectors were in consideration for the next generation kaon decay experiment. CALOR89 [11] based Monte Carlo simulations of several plug configurations were performed to understand contributions of neutrons (n), photons (γ), and charged (c) particles to chamber rates. Neutrons were simulated to strike the plug with the appropriate spectrum and beam divergence and the resulting hadronic cascade was simulated down to cutoff kinetic energies of 10 KeV for electrons, 2 KeV for photons, and thermal energies for neutrons. The magnet iron and coils were included in the simulation, but no attempt was made to simulate the drift chamber response. Instead the number of interactions in the drift chamber were calculated by weighting each n, γ, or c track that crossed the drift chamber by the probability of interaction. Interactions on hydrogen only were considered relevant for neutrons and the tabulated cross section was used [5]. Attenuation lengths from the PDG [12] were used for photons. Charged particles were accounted to always produce an interaction in the chambers. Similar estimates of drift chamber rates were also possible using the Bonner sphere and liquid scintillator measurements of n, γ, and c fluxes. The measurements, however, had to be corrected by Monte Carlo because the Bonner sphere and

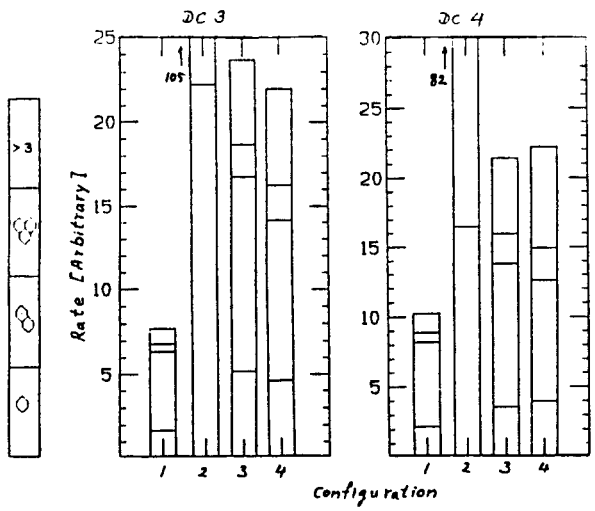

Fig. 6. Categorization of singles rate in upstream (DC3) and downstream (DC4) drift chambers for different plug configurations. The bar on left shows the different categories. Configurations are 1) No plug, 2) bare metal plug, 3) fully shielded plug, 4) fully shielded plug with an extra inch of tungsten and polyethylene. The magnetic field was off for these measurements. Large fraction of the rate was due to positively charged particles and the magnetic field produced asymmetries on the two sides of the plug that reflected this fact.

liquid scintillator detectors did not provide any directional information, and so the amount of material traversed could not be calculated properly. Furthermore, these detectors were not in the same locations as the drift chambers. Essentially the measurements were used to provide an absolute scale for n, γ, and c induced rates. Finally for comparison with data, groups of adjacent wires hit (clusters) in the drift chambers were defined to be a single particle interaction. To obtain only the plug induced hit rates, rates measured without the plug were subtracted with appropriate weights. Tables 2 and 3 give the results of this analysis.

CONCLUSION

After much experimentation we are confident that we can design a beam dump and predict changes in the drift chamber singles rate due to changes in the shielding material. Since much of this knowledge can be applied towards SSC experiments I have made a list of several ideas that we learned while designing the plug.

- Appropriate geometrical design and use of polyethylene can reduce neutron induced rates by a large factor. The tunnel in the front of the plug moved the core of the hadronic shower away from the front chambers thus reducing the solid angle extended by the front chambers.

- The total predicted Monte Carlo rates are within a factor of two of the actual drift chamber rates and large changes in one seem to track with large changes in the other. The Monte Carlo is only consistent within a factor of two with the measurements from the drift chambers and the liquid scintillator and Bonner sphere detectors. A combination of incomplete measurements, uncertain normalizations, and modeling errors in the code itself are all responsible at some level for the difference. If we trust the Monte Carlo results at face value then, for the shielded plug, nearly half of the drift chamber rates are caused by charged particles and about 20% are due to photons.

- The Monte Carlo predicts 2-4 times as much neutron-induced drift chamber rate as we measure with the Bonner spheres. The neutron energy spectra, shown in figures 4-5, have similar shapes

above 1 KeV but there are just more neutrons per bin from the Monte Carlo. The region below 1 KeV does not agree as well. This might be due to the Bonner sphere unfolding code which does not have enough constraints from data in that region.

- The comparison of photon-induced rate shows reasonable agreement between the Monte Carlo and the measurements using the liquid scintillators. Furthermore, the photon rates are highly correlated with the neutron rates.

	Metal only plug	Shielded plug	Extra 1" W and poly
DC3 rate - pre-plug	**3315**	**772**	**545**
Monte Carlo charged particles	987	339	242
neutrons	1125	247	70
photons	235	137	94
Sum	**2347**	**783**	**406**
Liquid scintillator and Bonner spheres minus pre-plug charged particles	401	158	195
neutrons	432	99	31
photons	205	100	53
Sum	**1038**	**357**	**279**

Table 2. Comparison of drift chamber DC3 rates (in clusters/beam telescope count) from charged particles, neutrons, and photons as predicted by the Monte Carlo simulations and the liquid scintillator and Bonner sphere measurements.

	Metal only plug	Shielded plug	Extra 1" W and poly
DC4 rate - pre-plug/2	**2542**	**654**	**624**
Monte Carlo charged particles	215	202	114
neutrons	1025	195	55
photons	187	110	59
Sum	**1427**	**507**	**228**
Liquid scintillator and Bonner spheres minus pre-plug/2 charged particles	409	504	263
neutrons	263	48	21
photons	240	78	38
Sum	**912**	**630**	**322**

Table 3. Comparison of drift chamber DC4 rates (in clusters/beam telescope count) from charged particles, neutrons, and photons as predicted by the Monte Carlo simulations and the liquid and Bonner sphere measurements.

I thank Jim McDonough and the Texas group for helping me understand their work on the analysis of the plug and for help in preparing this presentation. I also thank Charlene Macik for preparing the manuscript.

REFERENCES

[1] AGS proposal 871, 1990. The collaborators on the phase of the experiment reported here are: W. R. Molzon, A. Heinson, M. V. Diwan, K. Eckland, G. M. Irwin, K. Lang, D. A. Ouimette, A. J. Schwartz, S. G. Wojcicki, J. Belz, C. M. Guss, V. L. Highland, S. H. Kettell, W. K. McFarlane, G. W. Hoffmann, J. McDonough, S. Worm, B. Ware, P. J. Riley, J. L. Ritchie, A. Yamashita, M. Eckhause, A. D. Hancock, J. R. Kane, Y. Kuang, W. F. Vulcan, R. E. Welsh, R. G. Winter, M. Witkowski.

[2] A. P. Heinson, et al., Phys. Rev. D 44, R1 (1991).

C. Mathiazagan, et al., Phys. Rev. Lett 63, 2185 (1989).

J. Urheim, PhD thesis (unpublished), University of Pennsylvania, 1989.

[3] P. Buchholz, K. McFarlane, internal note KL-268 (1989). This measurement determined the neutron flux to be between (4 - 8) $\times 10^8$ n/Tp; C. Milner, internal note KL-256, a neutron activation measurement gives 3.8×10^8 n/Tp. The number used in this paper 3.5×10^8 n/Tp has a 30% systematic error.

[4] J. R. Sanford and C. L. Wang, BNL - 11479, 1967.

[5] D. I. Garber and R. R. Kinsey, NBL - 325, 1976.

[6] "Design of a compact beam dump for the BNL - AGS neutral beam", E871 collaboration, to be published in NIM.

[7] R. L. Bramblett, R. I. Ewing, T. W. Bonner, NIM, V9, Oct. 1960. pp [1-12

[8] K. A. Lowry and T. L. Johnson, NRL Memorandum Report 5340, 6 June 1984.

[9] C. L. Morris et al., NIM 137 (1976) pp 397-398.

[10] W. R. Burrus, NIM 67 (1969) pp 181-196.

[11] T. A. Gabriel, . Bishop, F. S. Alsmiller, R. G. Alsmiller, J. O. Johnson, ORNL/TM-11185 (1989).

[12] K. Hikasa, et al., Physical Review D 45, (1992).